



The use of calcium alginate-activated carbon composite material in fixed-bed columns for methylene blue removal from wastewater

Ahmed Boucherdoud^{a,b}, Benaouda Bestani^{a,*}, Nouredine Benderdouche^a, Laurent Duclaux^c

^aLaboratoire de Structure, Elaboration et Application de Matériaux Moléculaires, SEA2M, Faculté des sciences et de la technologie.-Université Abdelhamid Ibn Badis -Mostaganem, Algérie; emails: bo-ahmed@live.fr (A. Boucherdoud), bestanib@yahoo.fr (B. Bestani), benderdouchen@yahoo.fr (N. Benderdouche)

^bInstitut des Sciences Exactes et Sciences de la Vie, Centre Universitaire Ahmed Zabana, Relizane, Algérie

^cLaboratoire de Chimie Moléculaire et Environnement (LCME), Université de Savoie, Mont Blanc, Chambéry F-73000, France; email: laurent.duclaux@univ-smb.fr

Received 2 April 2018; Accepted 11 March 2019

ABSTRACT

Four calcium alginate (ALG)-activated carbon (AC) composites were prepared by ionic gelation method using calcium alginate and Merck activated carbon at different ratio ALG/AC ranging from 1/1 to 1/4. The obtained spherical beads samples were characterized by scanning electron microscopy, zero point of charge (pH_{ZPC}) and Fourier transform infrared spectrometry spectroscopy and tested for methylene blue removal from aqueous solutions in continuous mode. The bed depth service time model adequately described methylene blue adsorption onto the prepared composites. Parameters effecting breakthrough curves such as bed depth, flow rate and inlet dye concentration were investigated using Adams–Bohart, Thomas, and Yoon–Nelson models which showed good fit for the breakthrough curves. It has been found that the amount of adsorbed dye decreases with increasing ALG/AC ratio and C_i/C_0 values reaching a maximum value of 40.70 mg/g. Adsorption through a packed bed column is a feasible and economical technique for the removal of dyes. We can conclude that the composite material of calcium alginate and activated carbon can effectively be used to remove dyes from wastewater.

Keywords: Adsorption; Composite; Calcium alginate; Methylene blue; Fixed bed column

1. Introduction

Industrial activities in the last decades have increasingly threaded not only the environmental but also had a negative impact on aquatic life and human health [1]. In particular, dyes used extensively in textile industry, in the paper, rugs, printing, leather, and food represent a highly visual class of pollutants [2–4]. Not easily biodegradable, most synthetic dyestuffs are resistant to environmental conditions due to their complex aromatic structures, they are toxic to aquatic life, carcinogenic, mutagenic and can affect

of seriously human health by damaging vital organs once discharged directly without any prior treatment [5]. In this study, methylene blue dye has been chosen as adsorbate molecule, because it is widely used in industry for dyeing cotton, wood and silk [6] and also can be easily be removal from wastewater by most adsorbents [7]. When released in the environment, it can generate health disease to human and animals such vomiting, diarrhea, and eyes injuries [5]. Hence, it is desirable to remove methylene blue-causing contaminants from effluents before its discharge into the natural environment. Several techniques have been proposed for dyes removal from wastewater such as, Chemical and

* Corresponding author.

physical like degradations, flocculation, coagulation, and ion exchange [8–10]. The adsorption on a solid adsorbent remains a technique of choice because of its simplicity, ease of use and the low costs. As a solid, activated carbon (AC) is an adsorbent widely used because of its well-defined chemical and textural properties among other adsorbents. Activated carbons prepared from many wastes as precursors applied to methylene blue (MB) removal from liquid effluents have been largely reported in the literature [11–14], but limited to batch processes in a simple stirring vessel. In this paper research, continuous mode (fixed-bed column) was used to remove the above-mentioned dye as largely adopted in industrial scale [15,16]. Commercial activated carbon from Merck encapsulated in sodium alginate at different ratios was used as an adsorbent for this purpose.

Sodium alginate is a substance is a natural polymer composed of two monomeric units, β -D-mannuronic acid and α -L-guluronic acid. It is a biocompatible substance and nontoxic, recognized as safe by the food and drug administration, it is highly viscous and is often used as an emulsifier and is responsible for the exchange property as a gelling agent [17,18]. These properties give sodium alginate a variety of uses in many industries such as paint, dye thickener and can remove effectively heavy metal toxins from the bloodstream when used in specified doses. It is extensively used in titanium nanoparticles, magnetite nanoparticles [19,20] and activated carbon immobilization [21]. Several materials have been used to synthesize encapsulated nanoparticles for functional adsorbents development in order to remove methylene blue and other dyes [22,23]. Due to their biodegradable behavior, non-toxic, less expensive and possessing significant pollutants adsorption capacity, calcium alginate-activated carbon composite materials are the preferred one compared to TiO_2/CS (Chitosan) nanocomposites (63.58% removal) [24], gum/ Al_2O_3 nanocomposite (90% removal) [19], $\text{Ag}/\text{CeO}_2/\text{ZnO}$ nanostructure (98% removal) [25] and Chitosan–clay composite [26]. In addition the prepared material is cheap and uses non-toxic chemical compared to the resin [27]. It is also regenerable and biodegradable, compared to the nano-composite prepared with metals such as chitosan- SnO_2 [28], nanosized yttrium doped CeO_2 [29] and Fe_3O_4 -Trisodium citrate nanocomposite [30]. Effect of ALG/AC ratios on methylene blue adsorption in continuous mode was the aim of this study since for most applications, continuous flow saves time, energy, costs and can increase productivity. It can also be more effective than batch processing.

2. Materials and methods

2.1. Materials

Chemical reagents: Sodium alginate (91% purity) from LOBA Chemie Pvt. Ltd. (India), Activated carbon from Merck (Germany), Calcium chloride from Sigma Aldrich (USA) and methylene blue from Merck (dye content $\geq 85\%$) used in this study were of analytical grade.

Stock solutions with known concentrations were prepared according to standard procedure by dissolving the required amount of methylene blue in distilled water. Successive dilutions were used to obtain working solutions

of the desired concentrations. Table 1 summarizes some important characteristics of the studied dye.

2.2. Preparation of composite beads ALG/AC

The composite beads alginate-activated carbon (ALG/AC) was prepared by ionic gelation method. Exact amount of powdered activated carbon ranging from 1.0 to 4.0 g was dispersed in 100 mL of deionized water, stirred until a clear homogeneous solution is obtained. The solution was added slowly to 100 mL of sodium alginate (1%, w/v) and the mixture was stirred for 2 h. Once the mixture was homogenous, 250 mL of calcium chloride solution (2 wt.%) was added using a peristaltic pump at a flow rate of 4 mL/min. The all was gently stirred to prevent any agglomeration. Composite beads were instantaneously formed in the gelation bath and cross-linked for 15 min. Finally, we get composite beads at different ALG/AC ratio (1/1, 1/2, 1/3, and 1/4).

2.3. Samples characterizations

Fourier transform infrared spectrometry (FTIR) was performed on KBr discs (approximate weight fraction of 0.1%) using an attenuated total reflectance platinum Diamond 1 Refl spectrometer on composite beads samples to identify the functional groups responsible for the chosen dye uptake. Measurements were performed in the wave number range of $4,500\text{--}400\text{ cm}^{-1}$ at 1 cm^{-1} spectral resolution.

Scanning electron microscopy-energy dispersive X-ray (SEM-EDX) spectroscopy was used to observe the samples' topography and to identify and to localize elements at the surface of the materials composite beads by phase contrast. The scanning electron microscopy (SEM) analysis was used to facilitate the analysis of specific zones at the surface of different composite beads. This was done using an environmental SEM HIROX SH 400 M SEM-EDS Bruker apparatus.

The zero point of charge (pH_{zpc}) defined as the absence of both positive charge (required by adsorbent surface due to H^+ adsorption at low pH) and negative one (required by adsorbent surface due to H^+ release at high pH values). It is of fundamental importance in carbon surface characterization since it measures the carbon's acidity/basicity at which the surfaces charge density is zero [31,32].

pH_{zpc} was determined as follows: 50.0 ± 0.1 mL of a 0.01 ± 0.01 M aqueous solution of NaCl was placed in each of a series of stoppered conical flasks. The initial pH (pH_i) of the solution in each flask was adjusted (from 2 to 12) using 0.01 ± 0.01 M HCl or NaOH, respectively, following which 0.15 ± 0.01 g of activated carbon was added to each flask and

Table 1
Chemical structure and characteristics of adsorbed dye

CI	52015
Molecular formula	$\text{C}_{16}\text{H}_{18}\text{ClN}_3\text{S}_3\text{H}_2\text{O}$
Molecular weight (g mol^{-1})	373.90
Maximum wavelength (λ_{max})	665
Supplier	Merck
CAS number	7220-79-3
Water solubility (g/L)	44

the resulting suspensions stirred for 48 h then the final pH (pH_i) value was measured Methylene blue outlet concentration was determined by measuring the absorbance at 664 nm with JENA-UV-visible spectrophotometer.

2.4. Experimental procedure

The fixed-bed columns experiments were made of glass tube of 17 mm inner diameter and 200 mm height at ambient. Both column ends are connected using silicone tubing for sucking Methylene blue solution which is continuously fed to the fixed bed of composite beads at room temperature using a peristaltic pump. The treated samples collected on the output of the measured time intervals. As long as the outlet solution concentration is below the upper limit, its purification is taking place.

The experiments were performed by varying the bed height (5, 10, and 15 cm), the initial concentration of methylene blue solution (100, 200, and 300 mg L⁻¹) and the flow rate (4, 6, and 8 mL min⁻¹) for different composite beads as shown in Table 2. In order to remove traces of methylene

blue, the column was flushed with distilled water prior to each experiment.

3. Results and discussion

3.1. Composite beads characterization

Before testing the prepared composite beads for methylene blue removal from aqueous solutions in continuous mode, samples were characterized as follow:

3.1.1. Infrared characterization

FTIR analyses were performed for all samples. Analysis of the measured IR spectra (Fig. 1) show characteristic peaks at 3,244 cm⁻¹ due to OH⁻ stretching. At 1591 and 1,405 cm⁻¹ strong bands assigned to the symmetric and anti symmetric stretching vibration of the carboxyl group (COO⁻), strong band at 1,024 cm⁻¹ related to C–O–C anti symmetric stretching. Other peaks were detected around 2,914 cm⁻¹ related to aliphatic C–H vibrations. Low intensity peak at 3,720 cm⁻¹ and 2,323 cm⁻¹ reveals to the presence of amine function (N–H bonds) and nitrile function C≡N, a weak band at 2,046 cm⁻¹ represents the elongation of alkyne function C≡C, band at 815 cm⁻¹ relating to the deformation out of the plane of group =C–H, After adsorption spectrum (e) shows an appearance of three peaks at 1,392 cm⁻¹ attributed to aromatic CN, 799 cm⁻¹ corresponds to the group C–S and 554 cm⁻¹ corresponds to the C=C aromatics

3.1.2. Surface morphology characterization

Fig. S1 shows SEM giving a general surface morphology images for the different composite beads with a granular morphology of rough and irregular spherical shape (Fig. S2) due to crosslinking between different polymer chains. For all studied ALG/AC ratios, we have noticed the existence of

Table 2
Fixed bed properties and operating conditions

Composite beads	Bed height (cm)	Flow rate (mL/min)	Inlet concentration (mg/L)
ALG/AC (1/1)	5	6	100
		10	100
	10	4	100
			200
			300
		8	100
			100
			100
	15	6	100
		5	6
10			100
ALG/AC (1/2)	5	6	100
		10	100
	10	4	100
			200
			300
		8	100
			100
			100
	15	6	100
		5	6
10			100
ALG/AC (1/3)	5	6	100
		10	100
	10	4	100
			200
			300
		8	100
			100
			100
	15	6	100
		5	6
10			100
ALG/AC (1/4)	5	6	100
		10	100
	10	4	100
			200
			300
		8	100
			100
			100
	15	6	100

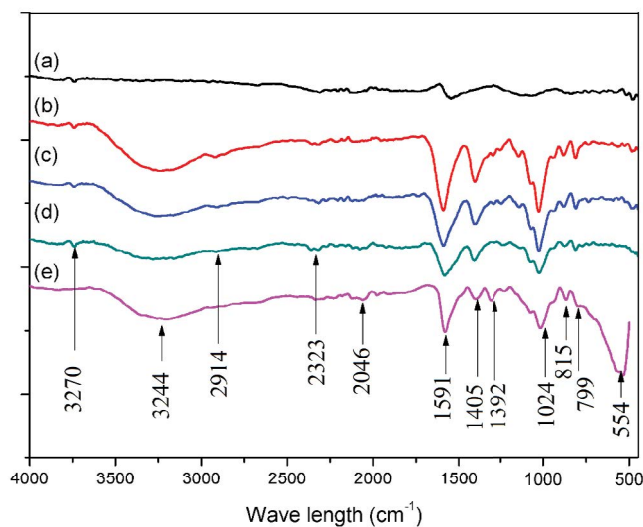


Fig. 1. FTIR spectrum of (a) Merck activated carbon and their composite beads at different ratio ALG/AC (1/1), (b) ALG/AC (1/2), (c) ALG/AC (1/3), (d) ALG/AC (1/4), and (e) after methylene blue adsorption.

small particles agglomeration due to the calcium chloride solution impregnation. Particles amount is more important with the ratio 1/4 and become low with the increasing ALG/AC ratio which is confirmed by a high percentage of calcium relative to carbon for the ratio 1/4 on the EDX spectrum (27.19% C, 10.20% Ca) otherwise the ratios 1/3 and 1/4 shows a porous structure with large pores confirmed by a good adsorption capacity. Energy-dispersive (EDS) X-ray spectrum (Fig. S1) show a high percentage of oxygen for the ratios 1/1 and 1/2 (61.93%, 56.74%) confirms in the FTIR analysis by an intense band relative to (OH) groups. Higher carbon values are noticed in the 1/3 and 1/4 ratios (38.54%, 44.6%) compared to 1/1 and 1/2 ratios (27.19%, 28.97%), respectively. The percentage of Ca varies between (10%–16%) and the percentage of Na does not dissect 1.29% for all samples

3.1.3. The point of zero charge

The difference between initial (pH_i) and final (pH_f) values (ΔpH = pH_i - pH_f) was plotted against pH_i. The intersection point of the resulting curve shown in Fig. 2 with the abscissa, at which ΔpH = 0, gave the point of zero charge values of the samples before and after encapsulation with the sodium alginate [33,34].

As shown in Fig. 2 (ratio (1/4) case) there is increase in pH value from 6.85 to 8.7 due to the effect of the alkaline media of the sodium alginate presence after encapsulation.

3.2. Column studies

Continuous adsorption study in fixed-bed column system was expressed by the breakthrough curve plots. The later are simply represented by the ratio of outlet dye concentrations to their initial ones as a function of flow time (C_t/C₀ = f(t)) which are commonly used to provide information on parameters influencing in the functional column such as total adsorbed dye quantity q_{total} (mg) in the column calculated from Eq. (1)

$$q_{total} = \frac{Q}{1,000} \int_{t=0}^{t_{total}} C_{ad} dt \tag{1}$$

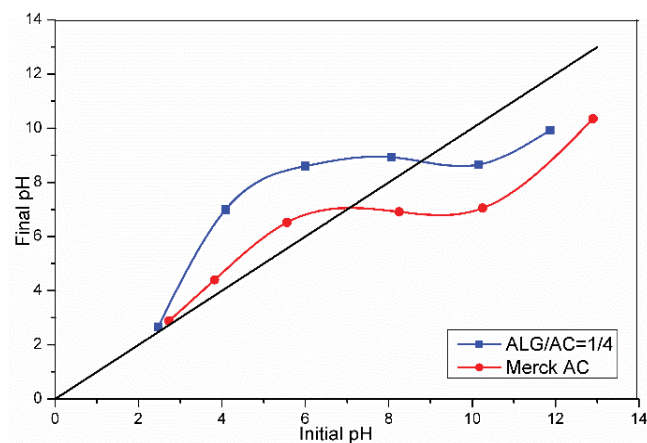


Fig. 2. pH drift plot of composite beads ALG/AC (1/4) and Merck activated carbon.

From which the equilibrium dye uptake (q_{eq}) in the column (or maximum adsorption capacity of the column) can be obtained as defined by Eq. (2)

$$q_{eq} = \frac{q_{total}}{m} \tag{2}$$

As the total amount of dye adsorbed (q_{total}) per g of sorbent (m) at the end of total flow time [35–37], the adsorption column capacity at 50% breakthrough time was calculated from q_{eq,(50%)} = ((breakthrough time) × (flow rate) × (feed concentration))/adsorbent mass).

3.2.1. ALG/AC ratio effect

Various experiments were performed to study the effect of ratio ALG/AC. During all tests, a flow rate of 6 mL/min, an inlet concentration of 100 mg/L and a bed height of 10 cm were kept constant, while ratios of ALG/AC were varied as follow: 1/1, 1/2, 1/3 and 1/4. Results are shown in Fig. 3. Saturation times of 152, 272, 376, and 488 min corresponding to different ALG/AC ratios used respectively were obtained at C_t/C₀ = 0.9. The break-through time increases with decreasing ALG/AC ratio while methylene blue uptake at equilibrium increased with decreasing the same ratios as mentioned in Table 3. The maximum adsorbed value of methylene blue at equilibrium obtained was 40.70 mg/g at ALG/AC ratio of 1/4.

3.2.2. Bed height effect

Since dye accumulation is largely dependent of the sorbents amount present in the column, bed height plays an important role in continuous adsorption process. Obtained breakthrough curves for the adsorption of methylene blue onto composite beads with different ALG/AC ratio (1/1 to 1/4) using various bed heights ranging from 5 to 15 cm at constant dye inlet concentration of 100 mg/L and constant flow rate of 6 mL/min are shown in Fig. 4.

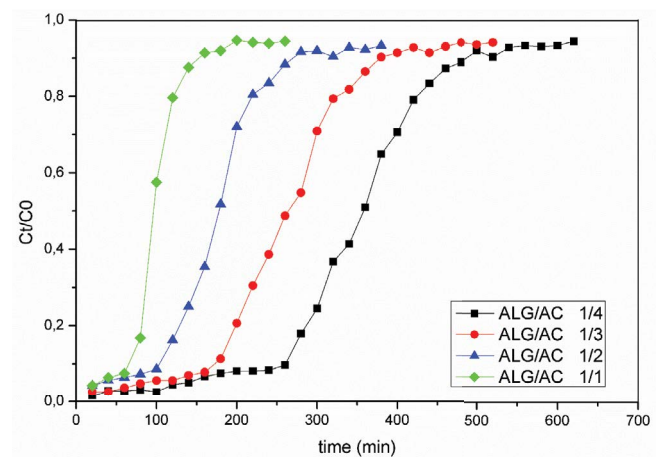


Fig. 3. Effect of ALG/AC ratios on breakthrough curves for methylene blue adsorption (Conditions: inlet concentration = 100 mg/L, bed height = 10 cm, flow rate = 6 mL/min and ambient temperature).

Table 3
Fixed-bed column adsorption capacity various ratio ALG/AC

Composite beads	Bed height (cm)	Initial dye concentration (mg/L)	Flow rate (mL/min)	Equilibrium uptake q_{eq} (mg/g)
ALG/AC 1/1	10	100	6	16.59
ALG/AC 1/2	10	100	6	24.25
ALG/AC 1/3	10	100	6	33.75
ALG/AC 1/4	10	100	6	40.70

As can be seen from the plots (Fig. 4) and values (Table 4), increasing bed height will increase the break through time. A higher adsorption rate was observed at higher bed height due to the increase in the composite beads mass resulting in mass transfer zone increase and providing then more binding sites for dye adsorption [38–40]. The proportionality between bed heights and adsorbent amounts would provide a larger service area leading to an increase in the volume of the treated solution [41]. In other words, methylene blue solution throughput volume is proportional to bed height, due to the availability of more number of sorption sites [42].

3.2.3. Feed flow rate effect

The effect of flow rate on methylene blue adsorption was conducted at different influent flow rates of 4, 6 and 8 mL/min, with constant inlet adsorbate concentration of 100 mg/L and adsorbent bed height of 10 cm as listed in Table 5. Fig. 5 shows the resultant breakthrough curves. At higher flow rate of 8 mL/min, the breakthrough occurred faster than the one exhibited by lower flow rate of 4 mL/min. That means that saturation occurs quickly at higher flow rates, while longer time is taken to reach saturation for lower flow rate resulting in more adsorption uptake [43,44].

3.2.4. Inlet dye concentration effect

The influence of adsorbate inlet concentration on the column performance was studied in the range of

Table 4
Column data and parameters with different bed height (Z) on the equilibrium uptake (q_{eq}) at 50% of C_i/C_0 and saturation time (t_s) for adsorption of MB onto composite beads

Composite beads	Z (cm)	C_0 (mg/L)	Q (mL/min)	t_s (min)
ALG/AC 1/1	5	100	6	140
	10	100	6	160
	15	100	6	180
ALG/AC 1/2	5	100	6	210
	10	100	6	280
	15	100	6	340
ALG/AC 1/3	5	100	6	300
	10	100	6	380
	15	100	6	480
ALG/AC 1/4	5	100	6	420
	10	100	6	500
	15	100	6	560

100–300 mg/L at constant bed height of 10 cm and flow rate of 6 mL/min. The breakthrough curves are illustrated in Fig. 6 and column operating parameters are presented in Table 6. We can see from C_i/C_0 plots (Fig. 6), that the composite beads were exhausted faster at more concentrated dye solutions for all studied cases in which the earlier breakthrough points were reached at higher concentration meaning that increasing inlet concentrations will decrease breakthrough points. This is due mainly to a decrease in adsorption zone length and then quick saturation of binding sites [45]. While latest breakthrough points were reached at lower inlet dye concentrations indicating that the mass transfer coefficient decreases (slowing transport) giving the possibility to the column the ability to treat a larger volume of solution [46,47].

A brief comparative literature survey concerning adsorption capacity of various nanocomposite adsorbents for methylene blue removal is shown in Table 7.

3.2.5. Bed depth service time

The Bed depth service time model is generally used not only to predict the relationship between bed depth (Z) and service time (t) but also to offer a simplest approach and rapid prediction of bed performance in terms of operating parameters and process concentrations.

This model provides useful data in changing operating parameters of an adsorption process by simply measuring beds adsorption capacities to different breakthrough values. The relationship between the break time and the bed height is given by Eq. (3)

$$\ln\left(\frac{C_0}{C_b} - 1\right) = \ln\left(\exp\left(\frac{KZN_0}{\vartheta}\right) - 1\right) - KC_0t \quad (3)$$

A linear relationship between bed-depth and service time may be given by Eq. (4)

$$t = \frac{N_0}{\vartheta C_0} Z - \frac{1}{KC_0} \ln\left(\frac{C_0}{C_b} - 1\right) \quad (4)$$

C_0 is the solute initial concentration (mg L⁻¹), C_b is the concentration of solute at breakthrough (mg L⁻¹), Z the column bed depth (cm), ϑ is the influent linear velocity (cm min⁻¹), N_0 the adsorption capacity per unit volume of fixed bed (mg mL⁻¹) representing the column saturation concentration, K is the adsorption rate constant (L mg⁻¹ min⁻¹) and t the column service time (min). Fig. 7 shows plots of t vs. Z will give a straight line with slope = $\frac{N_0}{\vartheta C_0} Z$ and

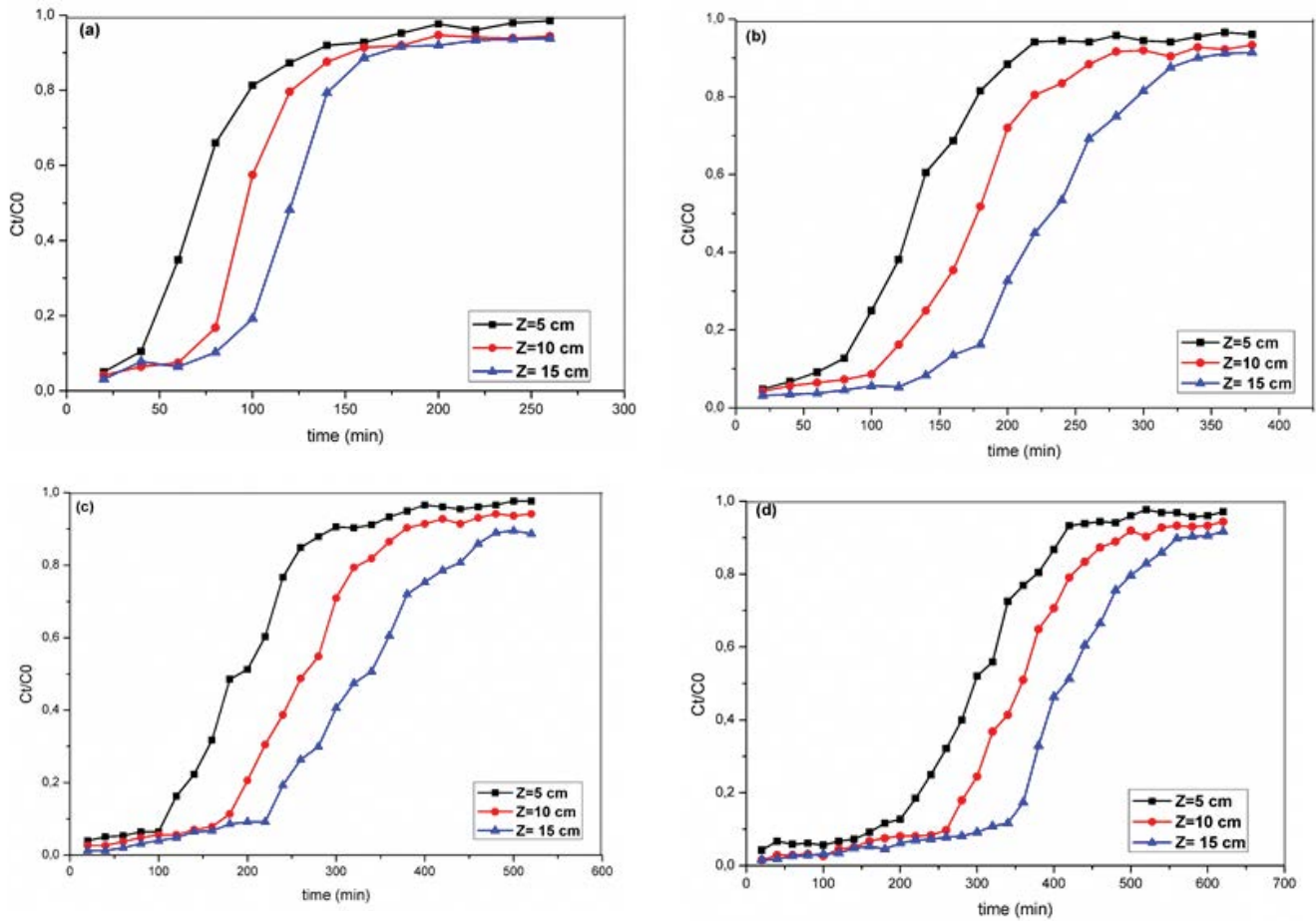


Fig. 4. Bed height effect on breakthrough curves at different ALG/AC ratio, (a) ALG/AC = 1/1, (b) ALG/AC = 1/2, (c) ALG/AC = 1/3, (d) ALG/A = 1/4. (Conditions: Inlet concentration = 100 mg/L, flow rate = 6 mL/min, room temperature).

an intercept = $\frac{1}{KC_0} \ln\left(\frac{C_0}{C_b} - 1\right)$ from which N_0 and K are respectively obtained.

Fig. 7 shows the effect of ALG / AC ratio on time (t) versus bed depth (Z) plots. The adsorbed dye amount increases with the decreasing ALG/AC ratio. The best adsorption capacity was obtained for 1/4 ratio which is 2.6 times higher than the 1/1 ratio. It can also be seen from Table 8 that the adsorption rate constant (K) decreases with increasing ALG/AC ratio.

From Fig. 8, it can also be said that the sorption capacity increases with increasing time because the adsorption capacity obtained at $C_t/C_0 = 0.9$ is greater than that at 0.2, and the rate constant K decreases with time as indicated in Table 9. With coefficients of determination greater than 0.99, the experimental data are well represented by the mathematical model.

4. Breakthrough data modeling

4.1. Application of Thomas model

Thomas model is one among many proposed mathematical models to describe the adsorption process in continuous mode [53]. It is based on the mass transfer

theorem which assumes that the pollutant diffuses through a liquid film around the surface of adsorbent particles. By its simplicity, this model is widely used to determine both the adsorbent maximum adsorption capacity and its rate constant needed in columns design [54]. The linearized form of Thomas model given by Eq. (5):

$$\ln\left(\frac{C_0}{C_t} - 1\right) = \frac{K_{Th}q_e m}{Q} - K_{Th}C_0 t \quad (5)$$

where C_t and C_0 are the concentrations of methylene blue solute (mg L^{-1}) at time (min) $t = t$ and $t = 0$, respectively; K_{Th} is the rate constant ($\text{L mg}^{-1} \text{min}^{-1}$), Q is the flow rate (L min^{-1}), q_e is the total adsorption capacity (mg g^{-1}), and m is the mass (g) of the adsorbent.

Fig. 9 shows that the experimental data were fitted this model in order to evaluate adsorbents maximum capacities (q_e) as a function of initial concentration keeping bed depth and flow rate constant. Values of K_{Th} , q_e and R^2 for the case of (ALG/AC = 1/4) ratio at the mentioned conditions are shown in Table 10. The adsorption capacity (q_e) strongly depends on influent concentration. It increases with increasing initial concentration, while the constant K_{Th} decreases. Same phenomena were reported in the literature [55,56].

Table 5

Effect of flow rate Q on equilibrium uptake ($q_{eq,50\%}$) and saturation time (t_s) for methylene blue adsorption onto composite beads

Composite beads	Q (mL/min)	C_0 (mg/L)	Z (cm)	t_s (min)	q_{eq} (50%)(mg/g)
ALG/AC 1/1	4	100	10	220	2.57
	6	100	10	160	3.20
	8	100	10	100	4.13
ALG/AC 1/2	4	100	10	300	4.83
	6	100	10	280	5.93
	8	100	10	240	6.77
ALG/AC 1/3	4	100	10	440	7.63
	6	100	10	380	8.77
	8	100	10	340	10.33
ALG/AC 1/4	4	100	10	540	10.76
	6	100	10	500	11.90
	8	100	10	420	13.67

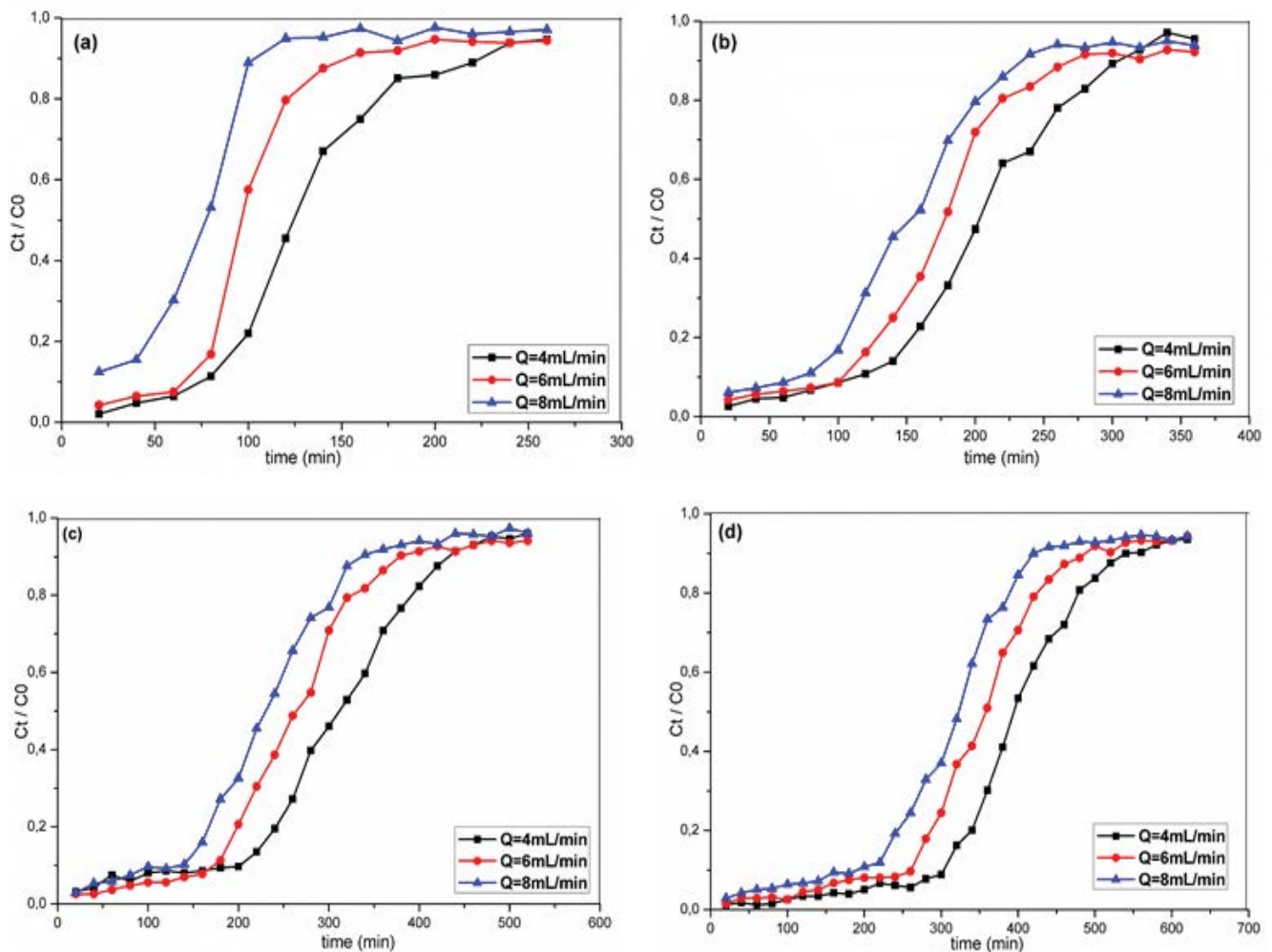


Fig. 5. Feed flow rate effect on breakthrough curves at different ALG/AC ratio, (a) ALG/AC = 1/1, (b) ALG/AC = 1/2 (c) ALG/AC = 1/3, and (d) ALG/A = 1/4. ([Inlet MB] = 100 mg/L, bed height = 10 cm, room temperature).

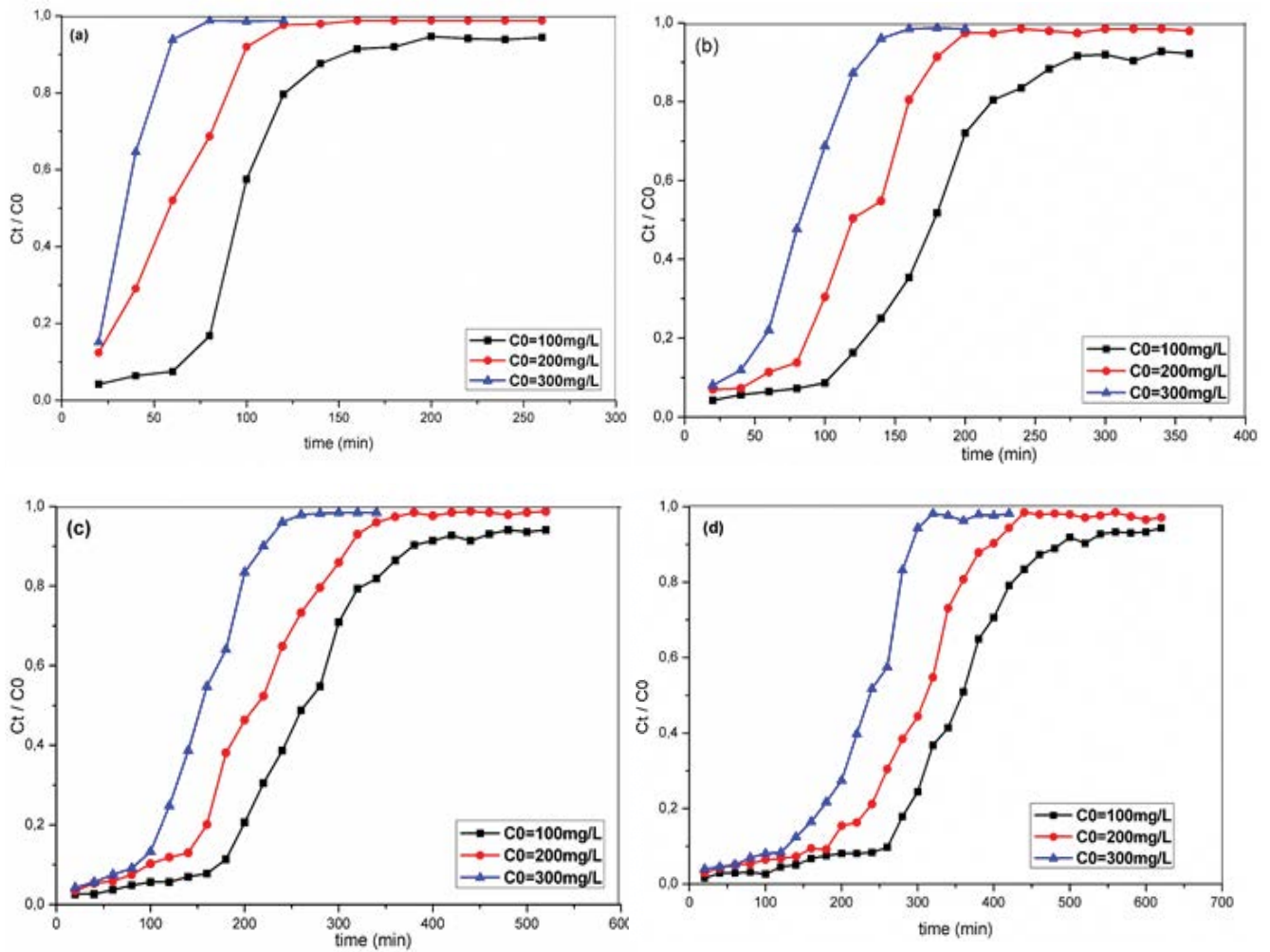


Fig. 6. Inlet concentration effect on breakthrough curves at different ALG/AC ratio, (a)ALG/AC = 1/1, (b) ALG/AC = 1/2 (c) ALG/AC = 1/3, and (d) ALG/A = 1/4. (Flow rate $Q = 6$ mL/min, bed height = 10 cm, room temperature).

Table 6

Effect of influent concentration on the equilibrium uptake ($q_{eq,50\%}$) and saturation time (t_s) for methylene blue adsorption onto composite beads

Composite beads	C_0 (mg/mL)	Q (mL/min)	Z (cm)	t_s (min)	$q_{eq(50\%)} (mg/g)$
ALG/AC 1/1	100	6	10	160	1.10
	200	6	10	120	1.93
	300	6	10	70	3.20
ALG/AC 1/2	100	6	10	280	2.73
	200	6	10	200	4.00
	300	6	10	160	5.90
ALG/AC 1/3	100	6	10	380	5.17
	200	6	10	360	7.06
	300	6	10	260	8.77
ALG/AC 1/4	100	6	10	500	7.83
	200	6	10	440	10.33
	300	6	10	320	11.87

4.2. Application of Adams–Bohart model

The Adams–Bohart model is used for the description of the initial part of the breakthrough curve ($C_t/C_0 = 0-0.5$) [57]. There is proportionality between the adsorption reaction rate, the adsorbent residual active sites and the adsorbate concentration. The equation of Adams–Bohart model in its linear form is expressed as follows [58]:

$$\ln\left(\frac{C_t}{C_0}\right) = K_{AB}C_0t - \frac{K_{AB}N_0Z}{v} \tag{6}$$

Table 7
Comparison of adsorption capacity of various nanocomposite adsorbents for methylene blue removal

Adsorbent	q_{max} (mg.g ⁻¹)	References
Activated lignin-chitosan blends	36.25	[48]
Chitosan nanocomposite beads	20.41	[49]
Stishovite-TiO ₂ nanocomposite	11.88	[50]
Fire clay-MnO ₂ nanocomposite	25.34	[51]
Graphene oxide/Ca alginate composites	181.81	[26]
Alginate-coated perlite beads	104.10	[52]
Alginate-activated carbon composite	40.70	This work

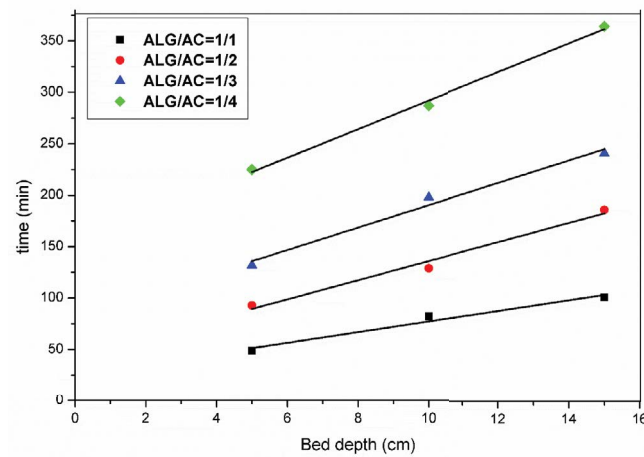


Fig. 7. Bed Depth Service Time at different ratio ALG/AC for methylene blue adsorption. (Conditions: $C_0 = 100$ mg/L, $Q = 6$ mL/min).

Table 8
Calculated BDST model constants for adsorption of methylene blue adsorption at different ALG/AC ratios (Conditions: $C_0 = 100$ mg/L, $Q = 6$ mL/min)

ALG/AC ratio	Equations	K ($\times 10^5$) (L/mg min)	N_0 ($\times 10^{-2}$) (mg/L)	R^2
1/1	$y = 5.2x + 25.33$	54.723	13.754	0.9764
1/2	$y = 9.3x + 43.00$	32.240	24.599	0.9833
1/3	$y = 10.9x + 81.33$	17.045	28.831	0.9854
1/4	$y = 13.9x + 153.00$	9.061	36.766	0.9961

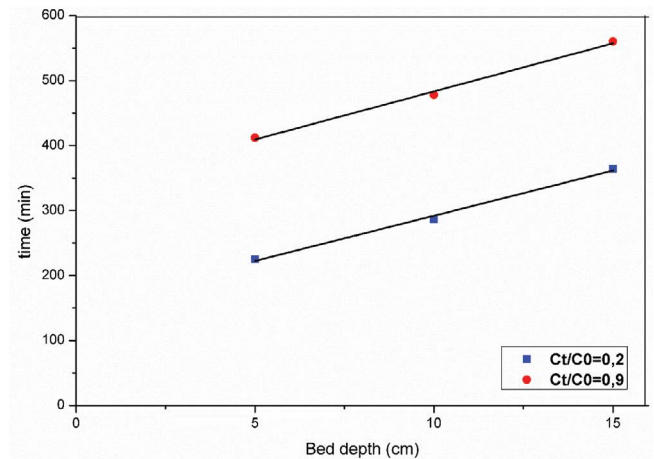


Fig. 8. Bed depth service time as a function of bed height for MB adsorption: case: 1/4 ratio, (Conditions $C_0 = 100$ mg/L, $Q = 6$ mL/min).

Table 9
Calculated BDST model constants for methylene blue adsorption of at different bed height for 1/4 ratio, (Conditions: $C_0 = 100$ mg/L, $Q = 6$ mL/min)

C_t/C_0	$K(\times 10^5)$ (L mg ⁻¹ min ⁻¹)	N_0 ($\times 10^{-2}$) (mg/L)	R^2
0.2	9.061	36.77	0.996
0.9	4.134	39.15	0.996

where K_{AB} is rate kinetic constant of Adams–Bohart model (L mg⁻¹ min⁻¹), v is the linear velocity (cm min⁻¹) and C_0 and C_t (mg/L) are the influent and effluent methylene blue concentrations. The values of K_{AB} and N_0 of this model shown in Table 10 were evaluated from the linear plot of $\ln(C_t/C_0)$ versus t as shown in Fig. 10.

The bed maximum adsorption capacity per unit volume of adsorbent increases with increasing inlet methylene blue concentration at fixed bed height and flow rate indicating a growth in N_0 values. While the kinetic constant K_{AB} decreases with increasing inlet concentration at the same K_{AB} conditions. These obtained values showed that increasing influent methylene blue concentration can lead to good column performance.

4.3. Application of Yoon–Nelson model

Based on the proportional probability relationship between the decrease rate of adsorption for each adsorbate

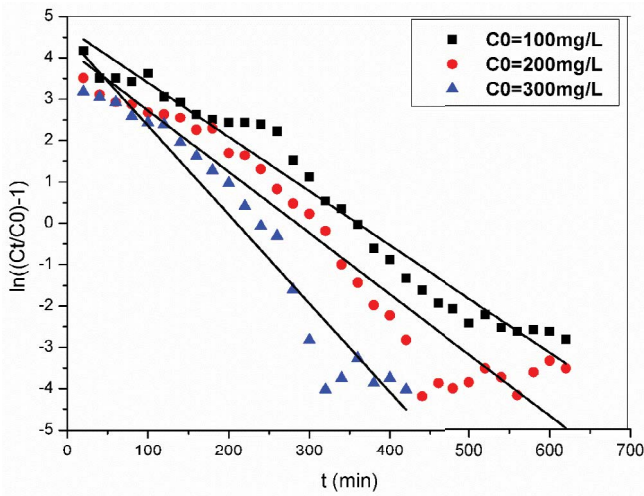


Fig. 9. Linear plot of Thomas model with experimental data at different inlet concentrations (Conditions: $Q = 6 \text{ L min}^{-1}$, $Z = 10 \text{ cm}$).

Table 10
Models parameters for methylene blue adsorption at (Conditions: $ALG/AC = 1/4$, $Q = 6 \text{ mL/min}$, $Z = 10 \text{ cm}$)

Model	Parameters	Influent concentration C_0 (mg/L)		
		100	200	300
Adams–Bohart	$K_{AB} (\times 10^5) \text{ (L/mg min)}$	7.50	3.20	3.13
	$N_0 (\times 10^{-2}) \text{ (mg/L)}$	92.18	175.01	186.33
	R^2	0.93	0.89	0.96
Thomas	$K_{Th} (\times 10^5) \text{ (L/mg min)}$	13.10	7.40	7.17
	$q_e \text{ (mg/g)}$	19.60	30.99	35.78
	R^2	0.96	0.93	0.94
Yoon–Nelson	$K_{YN} (\times 10^2) \text{ (1/min)}$	1.31	1.65	2.15
	$\tau \text{ (min)}$	359.17	276.11	209.34
	$\tau_{exp} \text{ (min)}$	356	310	237
	R^2	0.97	0.95	0.94

molecule, the adsorption amount and its breakthrough on the adsorbent, Yoon–Nelson model can be used to attenuate limitations of Adams–Bohart model of breakthrough curves in their ending period [58]. It is a simple theoretical curves that requires no data on adsorbent properties and physical characteristics of the adsorption bed used. The linear expression of Yoon–Nelson model is given by Eq. (7).

$$\ln\left(\frac{C_t}{C_0 - C_t}\right) = K_{YN}t - K_{YN}\tau \quad (7)$$

where $K_{YN} \text{ (min}^{-1}\text{)}$ is the rate constant and $\tau \text{ (min)}$ is the time required for 50% adsorbate breakthrough obtained from slope and intercept of $\ln(C_t/(C_0 - C_t))$ as a function of time t plots shown in Fig. 11. This model was applied to our experimental date in order to investigate the breakthrough

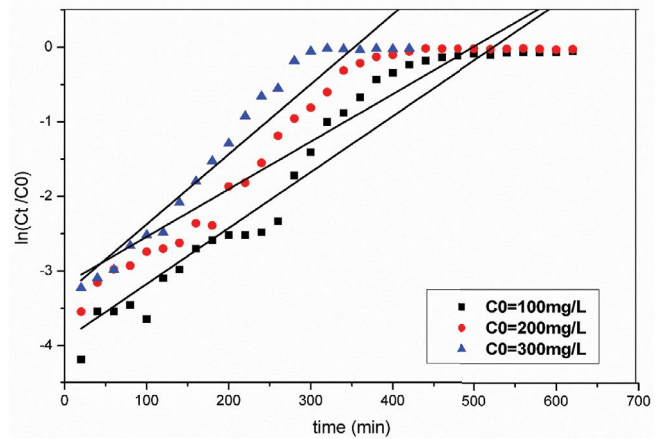


Fig. 10. Linear plot of Adams–Bohart model at different concentration (Conditions: $Q = 6 \text{ L min}^{-1}$, $Z = 10 \text{ cm}$).

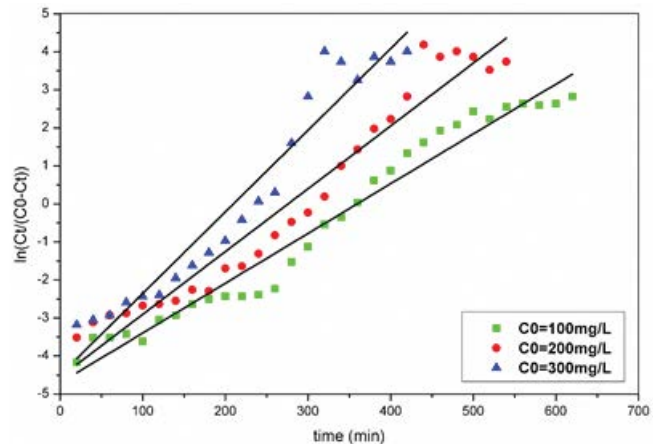


Fig. 11. Linear plot of Yoon–Nelson model with experimental data at different inlet concentration (Conditions: $Q = 6 \text{ L min}^{-1}$, $Z = 10 \text{ cm}$).

behavior of methylene blue through bed of composite beads at different inlet concentrations, flow rates and bed heights. For these two later, figures and values are not shown.

Values shown in Table 10 indicate that K_{YN} rate constant increases with the increasing inlet concentration of methylene blue at constant flow rate Q and bed height Z . Whereas, the τ values were found to decrease with increase in influent concentrations and there is a similarity between the calculated τ values and the experimental ones

At fixed flow rate and adsorbent mass, increasing influent concentration will increase K_{YN} values indicating then a narrower mass transfer zone and a greater mass transfer coefficient between phases and therefore, the adsorbate can easily be adsorbed. Since τ is related to the adsorbent capacity, greater capacity results in greater τ values which is the case in this study.

5. Conclusion

The prepared calcium alginate/activated carbon composites were found to be effective adsorbents for the

removal of methylene blue from aqueous solution at different variables such as influent concentrations, composite ALG/AC ratios, flow rates and bed heights. It is found that there is an increase of 82.55% (according to Thomas model) in adsorption capacity with increasing inlet concentration from 100 to 300 mg/L. Maximum uptake was obtained for ALG/AC ratio of ¼ and increasing bed height causes an increase in the saturation time by 3 times. Effects of bed depth and of flow rate on breakthrough curves were also investigated using Adams–Bohart, Thomas, and Yoon–Nelson models showing good fitting for all examined range of breakthrough curves at different influent concentrations and fixed flow rate and bed depth. Adsorption through a packed bed column is a feasible and economical technique for the removal of dyes.

Acknowledgements

Authors thank the financial support from National PRFU project (Université de Mostaganem) E00L01UN270120180003 A PARTIR DE 01/01/2018 of the Ministry of Higher Education, Algeria

References

- [1] Z. Aksu, S. Tezer, Biosorption of reactive dyes on the green alga *Chlorella vulgaris*, *Process Biochem.*, 40 (2005) 1347–1361.
- [2] Y. Akria, R.M. David, E. Philip, Proc. 21st Mid-Atlantic Conf. Ind. Waste, Harrisburg, PA, June 26–27, C.A. Cole, D.A. Long Eds., Technomic, Lancaster, PA, USA, 1989.
- [3] R. Perrin, J.P. Scharff, *Chimie industrielle*, 2eme Ed., Dunod, Paris, 1999.
- [4] S. Sirianuntapiboon, P. Srisornsak, Removal of disperse dyes from textile wastewater using bio-sludge, *Bioresour. Technol.*, 98 (2007) 1057–1066.
- [5] N. Douara, B. Bestani, N. Benderdouche, L. Duclaux, Sawdust-based activated carbon ability in the removal of phenol-based organics from aqueous media, *Desal. Water Treat.*, 57 (2015) 5529–5545.
- [6] M. BenallouBenzekri, N. Benderdouche, B. Bestani, N. Douara, L. Duclaux, Valorization of olive stones into a granular activated carbon for the removal of methylene blue in batch and fixed bed modes, *J. Mater. Environ. Sci.*, 9 (2018) 272–284.
- [7] M. Visa, Tailoring fly ash activated with bentonite as adsorbent for complex wastewater treatment, *Appl. Surf. Sci.*, 263 (2012) 753–762.
- [8] M. Mana, M.S. Ouali, L.C. DeMenorval, Removal of basic dyes from aqueous solutions with a treated spent bleaching Earth, *J. Colloid Interface Sci.*, 30 (2007) 9–16.
- [9] J. Panswed, S. Wongchaisuwan, Mechanism of dye wastewater colour removal by magnesium carbonatehydrated basic, *Water Sci. Technol.*, 18 (1986) 139–144.
- [10] M. Rafatullah, O. Sulaiman, R. Hashim, A. Ahmad, Adsorption of methylene blue on low-cost adsorbents, *J. Hazard. Mater.*, 177 (2010) 70–80.
- [11] H. Mittal, K. Vaneet, Saruchid, S.R. Suprakas, Adsorption of methyl violet from aqueous solution using gum xanthan/Fe₃O₄ based nanocomposite hydrogel, *Int. J. Biol. Macromol.*, 89 (2016) 1–11.
- [12] Z. Jia, Z. Li, S. Li, Y. Li, R. Zhu, Adsorption performance and mechanism of methylene blue on chemically activated carbon spheres derived from hydrothermally-prepared poly(vinyl alcohol) microspheres, *J. Mol. Liq.*, 220 (2016) 56–62.
- [13] O. Pezoti, Jr., A.L. Cazetta, P.A.F. Isis Souza, K.C. Bedin, A.C. Martins, L.S. Tais, V.C. Almeida, Adsorption studies of methylene blue onto ZnCl₂-activated carbon produced from buriti shells (*Mauritia flexuosa* L.), *J. Ind. Eng. Chem.*, 20 (2014) 4401–4407.
- [14] J.L. Gong, Y.L. Zhang, Y. Jiang, G.M. Zeng, Z.H. Cui, K. Liu, C.H. Deng, Q.Y. Niu, J.-H. Deng, S.Y. Huan, Continuous adsorption of Pb(II) and methylene blue by engineered graphite oxidecoated sand in fixed-bed column, *Appl. Surf. Sci.*, 330 (2015) 148–157.
- [15] R.P. Han, Y. Wang, X. Zhao, Y.F. Wang, F.L. Xie, J.M. Cheng, M.S. Tang, Adsorption of methylene blue by phoenix tree leaf powder in a fixed-bed column: experiments and prediction of breakthrough curves, *Desalination*, 245 (2009) 284–297.
- [16] A.F. Hassan, A.M. Abdel-Mohsen, M.G. MoustafaFouda, Comparative study of calcium alginate, activated carbon, and their composite beads on methylene blue adsorption, *Carbohydr. Polym.*, 102 (2014) 192–198.
- [17] Y. Liu, S. Chen, L. Zhong, G. Wu, Preparation of high-stable silver nanoparticle dispersion by using sodium alginate as a stabilizer under gamma radiation, *Radiat. Phys. Chem.*, 78 (2009) 251–255.
- [18] N.M. Mahmoodi, B. Hayati, M. Arami, H. Bahrami, Preparation, characterization and dye adsorption properties of biocompatible composite (alginate/titania nanoparticle), *Desalination*, 275 (2011) 93–101.
- [19] V. Rocher, J.-M. Siaugue, V. Cabuil, A. Bee, Removal of organic dyes by magnetic alginate beads, *Water. Res.*, 42 (2008) 1290–1298.
- [20] T.Y. Kim, H. J. Jin, S.S. Park, S.J. Kim, S.Y. Cho, Adsorption equilibrium of copper ion and phenol by powdered activated carbon, alginate bead and alginate-activated carbon bead, *Ind. Eng. Chem.*, 14 (2008) 714–719.
- [21] J. Goel, K. Kadirvelu, C. Rajagopal, V.K. Garg, Removal of lead (II) by adsorption using treated granular activated carbon: batch and column studies, *J. Hazard. Mater. B*, 125 (2005) 211–220.
- [22] A.N. Bezbaruah, S. Krajangpan, B.J. Chisholm, E. Khan, J.J. Elorza Bermudez, Entrapment of iron nanoparticles in calcium alginate beads for groundwater remediation applications, *J. Hazard. Mater.*, 166 (2009) 1339–1343.
- [23] L. Bai, Z. Li, Y. Zhang, T. Wang, R. Lu, W. Zhou, S. Zhang, Synthesis of water-dispersible graphene-modified magnetic polypyrrole nanocomposite and its ability to efficiently adsorb methylene blue from aqueous solution, *Chem. Eng. J.*, 279 (2015) 757–766.
- [24] F. He, D. Zhao, J. Liu, C.B. Roberts, Stabilization of Fe–Pd nanoparticles with sodium carboxymethyl cellulose for enhanced transport and dechlorination of trichloroethylene in soil and groundwater, *Ind. Eng. Chem. Res.*, 46 (2007) 29–34.
- [25] Y. Li, Q. Du, T. Liu, J. Sun, Y. Wang, S. Wu, L. Xia, Methylene blue adsorption on graphene oxide/calcium alginate composites, *Carbohydrate Polymers*, 95 (2013) 501–507.
- [26] M. Auta, B.H. Hameed, Chitosan–clay composite as highly effective and low-cost adsorbent for batch and fixed-bed adsorption of methylene blue, *Chem. Eng. J.*, 237 (2014) 352–361.
- [27] M.A. Khan, Z.A. AlOthman, M. Naushad, M.R. Khan, M. Luqman, Adsorption of methylene blue on strongly basic anion exchange resin (Zerolit DMF): kinetic, isotherm, and thermodynamic studies, *Desal. Water Treat.*, 53 (2013) 515–523.
- [28] V.K. Gupta, R. Saravanan, S. Agarwal, F. Gracia, M.M. Khan, J. Qin, R.V. Mangalaraja, Degradation of azo dyes under different wavelengths of UV light with chitosan–SnO₂ nanocomposites, *J. Mol. Liq.*, 232 (2017) 423–430.
- [29] A. Akbari-Fakhrabadi, R. Saravanan, M. Jamshidijam, R.V. Mangalaraja, M.A. Gracia, Preparation of nanosized yttrium doped CeO₂ catalyst used for photocatalytic application, *J. Saudi Chem. Soc.*, 19 (2015) 505–510.
- [30] A.A. Alqadami, M. Naushad, M.A. Abdalla, M.R. Khan, Z.A. AlOthman, Adsorptive removal of toxic dye using Fe₃O₄-TSC nanocomposite: equilibrium, kinetic, and thermodynamic studies, *J. Chem. Eng. Data*, 61 (2016) 3806–3813.
- [31] W. Lijuan, L. Jian, Removal of methylene blue from aqueous solution by adsorption onto crofton weed stalk, *Bio. Resour.*, 8 (2013) 2521–2536.
- [32] M.V. Lopez-Ramon, F. Stoeckli, C. Moreno-Castilla, F. Carrasco-Marin, On the characterization of acidic and basic surface

- sites on carbons by various techniques, *Carbon*, 37 (1999) 1215–1221.
- [33] A. Belayachi, B. Bestani, A. Bendraoua, N. Benderdouche, L. Duclaux, The influence of surface functionalization of activated carbons on dyes and metal ions removal from aqueous media, *Desal. Water Treat.*, 57 (2016) 17557–17569.
- [34] Y.S. Al-Degs, M.A.M. Khraisheh, S.J. Allen, N.A. Ahmad, Effect of carbon surface chemistry on the removal of reactive dyes from textile effluents, *Water Res.*, 34 (2000) 927–935.
- [35] P.C.C. Faria, J.J.M. Orfao, M.F.R. Pereira, Adsorption of anionic and cationic dyes on activated carbons with different surface chemistries, *Water Res.*, 38 (2004) 2043–2052.
- [36] N. Atar, A. Olgun, S. Wang, S. Liu, Adsorption of anionic dyes on boron industry waste in single and binary solutions using batch and fixed-bed systems, *J. Chem. Eng. Data.*, 56 (2011) 508–516.
- [37] V. Russo, D. Masiello, M. Trifuoggi, M. Di Serio, R. Tesser, Design of an adsorption column for methylene blue abatement over silica: From batch to continuous modeling, *Chem. Eng. J.*, 302 (2016) 287–295.
- [38] E.I. El-Shafey, N.F. Ali Syeda, S. Al-Busafi, H.A.J. Al-Lawati, Preparation and characterization of surface functionalized activated carbons from date palm leaflets and application for methylene blue removal, *J. Environ. Chem. Eng.*, 4 (2016) 2713–2724.
- [39] M.K. Mondal, Removal of Pb(II) ions from aqueous solution using activated tea waste: adsorption on a fixed-bed column, *J. Environ. Manage.*, 90 (2009) 3266–3271.
- [40] B. Ahmad Albadarin, C. Mangwandi, Ala'a H. Al-Muhtaseb, G.M. Walker, S.J. Allen, N.M. Mohammad Ahmad, Modelling and fixed bed column adsorption of Cr(VI) onto orthophosphoric acid-activated Lignin. *Chin. J. Chem. Eng.*, 20 (2012) 469–477.
- [41] Z.Z. Chowdhury, S.M. Zain, A.K. Rashid, R. Rafique, K. Khalid. Breakthrough curve analysis for column dynamics sorption of Mn(II) Ions from wastewater by using *Mangostana garcinia* peel-based granular-activated carbon. *J. Chem.*, 2013, Article ID 959761, 8 pages.
- [42] P. Sivakumar, P.N. Palanisamy, Adsorption studies of basic Red 29 by a non-conventional activated carbon prepared from *Euphorbia antiquorum* L. *Int. J. Chemtech. Res.*, 1 (2009) 502–510
- [43] A. Negrea, L. Lupa, M. Ciopec P. Negrea, Experimental and modelling studies on As (III) removal from aqueous medium on fixed bed column, *Chem. Bull. Politechnica Univ. (Timisoara)*, 56 (2011) 89–93.
- [44] J.T. Nwabanne, P.K. Igbokwe, Adsorption performance of packed bed column for the removal of Lead (ii) using oil palm fibre international, *J. Appl. Sci. Technol.*, 2 (2012) 106–115.
- [45] N. Azouaou, Z. Sadaoui, H. Mokaddem, Removal of lead from aqueous solution onto untreated coffee grounds: a fixed-bed column study, *Chem. Eng. Trans.*, 38 (2014) 151–156.
- [46] A.A. Ahmad, B.H. Hameed, Fixed-bed adsorption of reactive azo dye onto granular activated carbon prepared from waste, *J. Hazard. Mater.*, 175 (2010) 298–303.
- [47] S. Sadaf, H.N. Bhatti, S. Ali, K. Rehman, Removal of Indosol Turquoise FBL dye from aqueous solution by bagasse, a low cost agricultural waste: batch and column study. *Desal. Water. Treat.*, 52 (2013) 184–198.
- [48] A.B. Albadarin, M.N. Collins, M. Naushad, S. Shirazian, G. Walker, C. Mangwandi, Activated lignin-chitosan extruded blends for efficient adsorption of methylene blue, *Chem. Eng. J.* 307, No. 1 (2017) 264–272.
- [49] I. Rahmi, M. Irfan, Methylene blue removal from water using H₂SO₄ crosslinked magnetic chitosan nanocomposite beads, *Microchem. J.*, 144 (2019) 397–402.
- [50] V.T. Priyaa, V. Venkateswaran, Equilibrium and kinetic data and process design for adsorption of methylene blue onto Stishovite-TiO₂ nanocomposite, *Global J. Biol. Agric. Health Sci.*, 3 (2014) 102–111.
- [51] P. Balasubramaniam, V. Venkateswaran, A. Rathinavelu, Adsorption of methylene blue on to fire clay -MnO₂ nanocomposite materials, *Int. J. Res. Advent Technol.*, 6 (2018) 2753–2763.
- [52] Ş. Parlayici, Alginate-coated perlite beads for the efficient removal of methylene blue, malachite green, and methyl violet from aqueous solutions: kinetic, thermodynamic, and equilibrium studies, *J. Anal. Sci. Technol.*, 10 (2019) 4.
- [53] L. Conter, R. Knox, *Ground Water Pollution Control*, Lewis, New York, USA, 1986, p. 96.
- [54] H.C. Thomas, Heterogeneous ion exchange in a flowing system, *J. Am. Chem. Soc.*, 66 (1944) 1664–1666.
- [55] N. Sankararamakrishnan, A.K. Sharma, R. Sanghi, Novel chitosan derivative for the removal of cadmium in the presence of cyanide from electroplating wastewater, *J. Hazard. Mater.*, 148 (2007) 353–359.
- [56] Y. Long, D. Lei, J. Ni, Z. Ren, C. Chen, H. Xu, Packed bed column studies on lead(II) removal from industrial wastewater by modified *Agaricus bisporus*, *Bioresour. Technol.*, 152 (2014) 457–463.
- [57] P. Loderio, R. Herreo, M.E. Sastre de Vicentes, The use of protonated *Sargassum muticum* as biosorbent for cadmium removal in a fixed-bed column. *J. Hazard. Mater.*, 137 (2006) 244–253.
- [58] Y.H. Yoon, J.H. Nelson, Application of gas adsorption kinetics. I. A theoretical model for respirator cartridge service time, *Am. Ind. Hyg. Assoc. J.*, 45 (1984) 509–551.

Supplementary Information

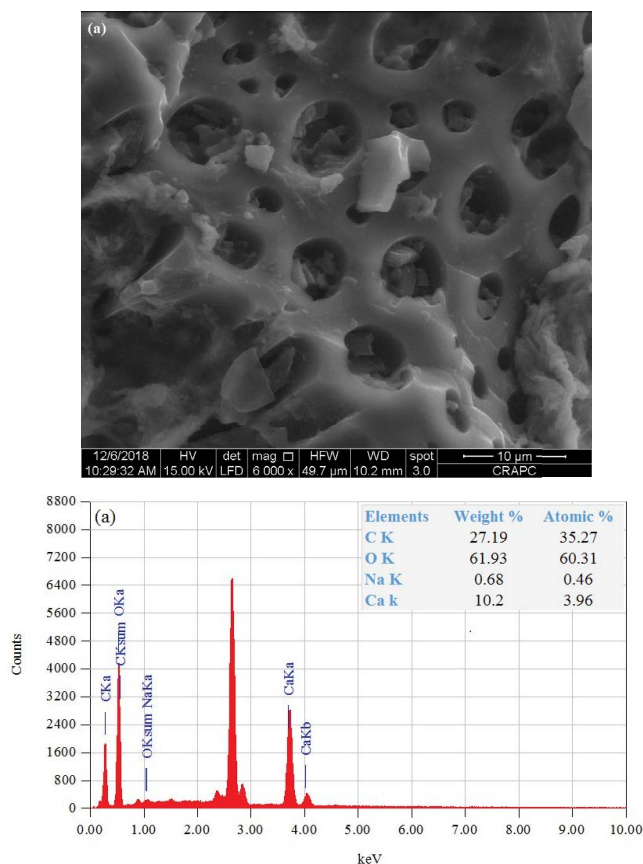


(Fig. S1 continued)

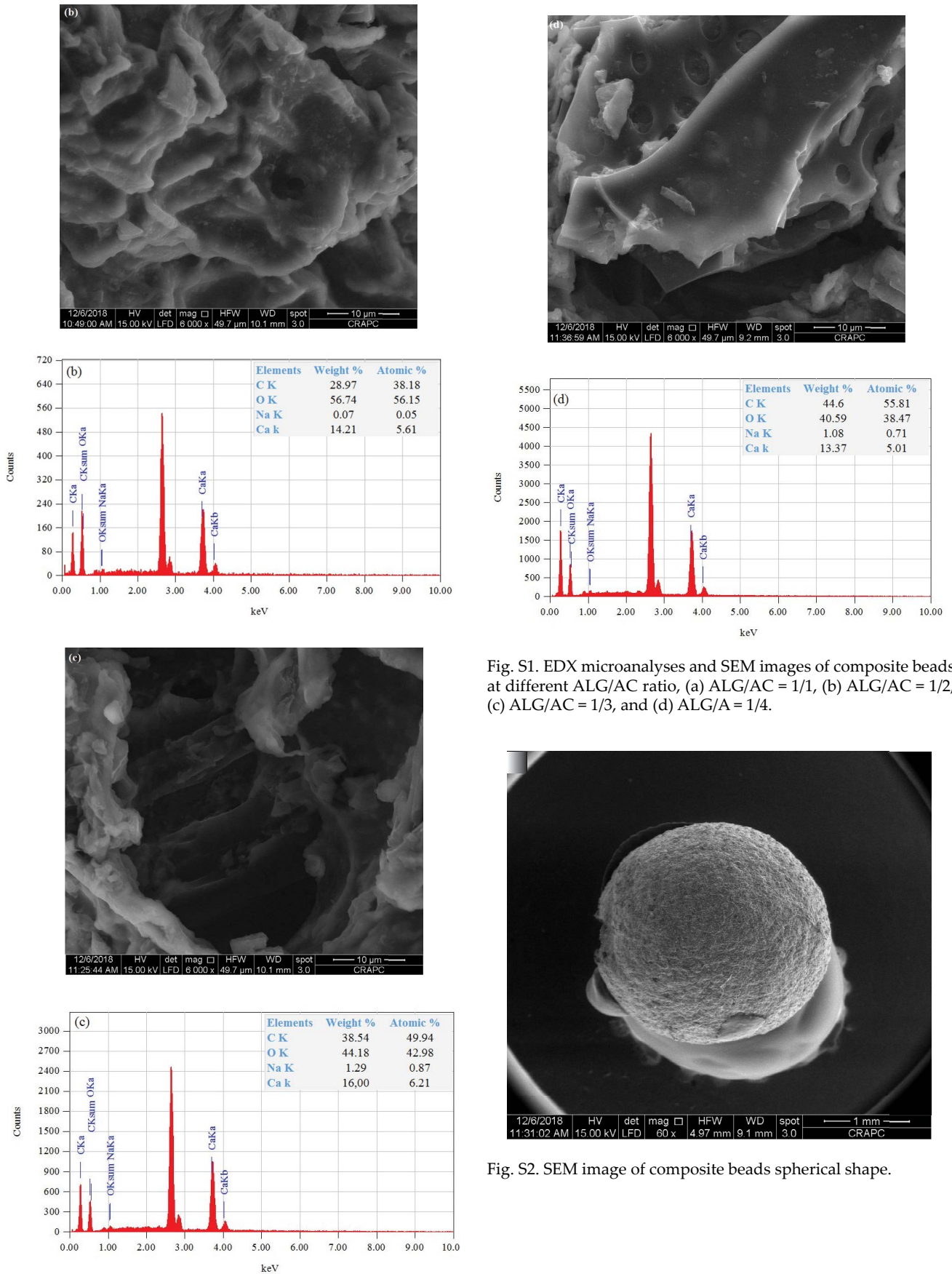


Fig. S1. EDX microanalyses and SEM images of composite beads at different ALG/AC ratio, (a) ALG/AC = 1/1, (b) ALG/AC = 1/2, (c) ALG/AC = 1/3, and (d) ALG/A = 1/4.

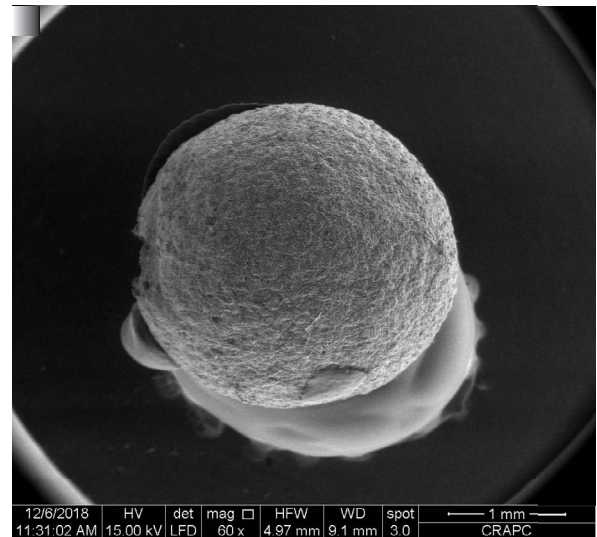


Fig. S2. SEM image of composite beads spherical shape.